

Congo red adsorption on metal-organic frameworks, MIL-101 and ZIF-8: kinetics, isotherm and thermodynamic studies

Cao Yang^a, Linling Yu^a, Rouxi Chen^b, Jianhua Cheng^{a,b,*}, Yuancai Chen^a, Yongyou Hu^a

^aMinistry of Education Key Laboratory of Pollution Control and Ecological Remediation for Industrial Agglomeration Area, School of Environment and Energy, South China University of Technology, Guangzhou 510006, China, Tel. +86-188-14116970, email: Aimee_yw@163.com (C. Yang), Tel. +86-020-38672029, email: chenyc@scut.edu.cn (Y. Chen), Tel. +86-203-9380506, email: ppyyhu@scut.edu.cn (Y. Hu)

^bSouth China Institute of Collaborative Innovation, Dongguan 523808, China, Tel. +86-203-8743625, Fax: +86-203-8743651, email: jhcheng@scut.edu.cn (J. Cheng)

Received 20 May 2017; Accepted 12 September 2017

ABSTRACT

In this study, MIL-101 and ZIF-8, two typical highly porous metal-organic framework materials, were synthesized using the simple one-pot methods for the adsorption of aqueous Congo red (CR). The study found that highly efficient removal of CR at neutral pH can be achieved with short contact time. The CR adsorption behaviors of the two adsorbents were studied and found to follow Langmuir isotherm and pseudo-second-order kinetic models. The maximum CR adsorption capacities of MIL-101 and ZIF-8 were up to 2248 and 1381 mg g⁻¹ at 298 K, respectively, significantly higher than most of the adsorbents previously studied. Especially, MIL-101 showed faster kinetics and higher adsorption capacity when compared to ZIF-8, which can be attributed to the larger porosity and pore size of MIL-101, and the direct coordination between the unsaturated metal sites in MIL-101 and CR. Thermodynamic studies suggested that the adsorption was a spontaneous and endothermic reaction. Additionally, MIL-101 and ZIF-8 showed good performance after regeneration. Therefore, as-prepared MIL-101 and ZIF-8 have great potential as adsorbents for wastewater treatment.

Keywords: Adsorption; Congo red; Metal-organic framework; MIL-101; ZIF-81

1. Introduction

Water pollution, especially due to dyeing wastewater, has received significant attention since several billion tons of dyeing wastewater are discharged from the textile industry annually [1]. Many dyes are stable, carcinogenic and difficult to biodegrade; hence, they can cause adverse human health impacts. Therefore, it is critical to develop techniques for the efficient removal of toxic dyes from contaminated water.

As a cost-effective and feasible method, the adsorption technology has wide applicability in wastewater treatment and has been extensively applied to the removal of various organic pollutants from water. Adsorbents such as silica [2], activated carbon [3], and zeolites [4] have been used for dye wastewater treatment because of their low cost and/or

abundance in nature. However, their adsorption capacity is quite limited, which can be due to low surface area or poor surface chemistry. Post-synthetic modification approaches have been used to enhance their efficiency for the removal of dyes, including magnetic MCM-41 silica particles grafted with poly (glycidylmethacrylate) brush [5], chitosan/polyvinyl alcohol/zeolite composite [6], Typha latifolia activated carbon/chitosan composite [7], etc. Though the dye adsorption capacity had improved, the wastewater treatment cost had also increased, limiting their use in practical applications. Therefore, it is important to develop adsorbents that are efficient, low cost, easy to synthesize, with adequate porosity.

Metal-organic frameworks (MOFs) have received increased research attention as novel porous crystalline materials due to their large surface areas, high porosities and tunable pore sizes. In the past few years, MOFs have been extensively studied for the adsorption of organic dyes

*Corresponding author.

from aqueous solution. For example, the maximum Congo red (CR) adsorption capacity of MIL-100(Fe) reached 714.3 mg g⁻¹ with a contact time of over 100 min [8]. Similarly, Cu-BTC had the adsorption capacity of 12.22 mg g⁻¹ for methylene blue in more than 40 min [9]. The uses of MIL-68 (In) nano-rods and ZIF-8 nanoparticles for the removal of aqueous CR have also been reported [10,11]. In these studies, it was noted that the time taken for adsorption equilibrium was long, and/or the adsorption capacity was not high. However, for practical dye wastewater treatment, the adsorbents should work at a neutral pH, and ambient temperature with short contact time.

Among the numerous MOFs, chromium based MIL-101 (MIL: Materials of Institute Lavoisier) and zinc based ZIF-8 (ZIF: Zeolitic Imidazolate Framework) were selected for this study. MIL-101, synthesized via a one-step hydrothermal process, is a mesoporous MOF with cubic structure, and possesses high specific surface area (ca. 4000 m² g⁻¹), high porosity (ca. 2.0 cm³ g⁻¹) and large pore size of about 2.9 and 3.4 nm [12]. Additionally, MIL-101 has a good chemical resistance to water, common solvents and high temperature [12,13]. ZIF-8, produced via a rapid room-temperature synthesis protocol, is a microporous MOF with sodalite structure, and holds permanent porosity, high thermal stability, and high chemical resistance to boiling alkaline water and organic solvents [14,15]. Due to these excellent properties, they have been widely studied for their potential applications in wastewater treatment [11,16,17]. In the previous studies, MIL-101, synthesized using the hydrofluoric acid-free method, has been used for the removal of CR and had a low adsorption capacity of 178.6 mg g⁻¹ for a dosage of 0.1 g L⁻¹ and initial CR concentration of 50 mg L⁻¹ [18]. Recently, Jiang et al. [11] also reported that CR adsorption onto ZIF-8, synthesized through hydrothermal reaction, took a long time to reach equilibrium, i.e., 100 min for an initial CR concentration of 80 mg L⁻¹ [11]. However, it is hypothesized that the performance characteristics of MIL-101 and ZIF-8 would be different if they are synthesized using different methods.

In this study, MIL-101 was synthesized with the addition of HF, while ZIF-8 was prepared at ambient conditions. The detailed synthesis methods and characterization of MIL-101 and ZIF-8 are described in this paper. Further, their adsorption performance for CR, which is a widely used azo dye, was investigated in detail for the first time, including adsorption kinetics, adsorption isotherms and thermodynamics. The adsorption mechanisms were also proposed to explain the excellent CR removal performance of MIL-101 and ZIF-8.

2. Materials and methods

2.1. Materials

Congo red was supplied by Tianjin Chemicals Co., Ltd., while chromium nitrate nonahydrate [Cr(NO₃)₃·9H₂O], terephthalic acid (H₂BDC), zinc nitrate hexahydrate [Zn(NO₃)₂·6H₂O] and 2-methylimidazole (MeIm) were purchased from Alfa Aesar China Co., Ltd. Hydrofluoric acid (HF, 48%) and methanol were supplied by Guangzhou

Chemicals Co., Ltd. All chemicals were used as received without further purification.

2.2. Synthesis of MIL-101 and ZIF-8

Typically, the synthesis protocol for MIL-101 was similar to the method followed by Ferey et al. [12]. Cr(NO₃)₃·9H₂O (2.0 g), H₂BDC (0.83 g), and HF (0.23 mL) were mixed with deionized water (24 mL) until complete dissolution occurred. The mixture was heated at 220°C for 8 h, and cooled in the atmosphere. MIL-101 powder was filtered from the solution, and washed with deionized water and ethanol. Finally, the resulting MIL-101 sample was collected and dried under vacuum at 150°C for 12 h. ZIF-8 was prepared following the method adopted by Zhang et al. [15] with slight modification. In summary, Zn(NO₃)₂·6H₂O (2.933 g) was used to obtain a mixture of Zn/MeIm/methanol with a molar ratio of 1:8:700. Stirring was stopped after the solution was mixed evenly, and left for aging for 1 h. The ZIF-8 samples were separated from the milky solution by centrifugation, washed with fresh methanol and dried at room temperature.

2.3. Characterization

The structural and morphological characteristics of the as-prepared MIL-101 and ZIF-8 samples were characterized using XRD, SEM, BET-N₂, XPS and TEM. The phases of the products were analyzed using powder X-ray diffraction (XRD) performed on a Bruker D8 Advance X-ray diffractometer operated at 40 kV and 40 mA with Cu K α radiation. The morphology was investigated by field emission scanning electron microscope (FESEM) with a MERLIN Compact instrument. The Brunauer-Emmett-Teller (BET) surface area was measured by the N₂ adsorption-desorption at 77 K with a Micromeritics ASAP2020 instrument. Pore size distribution was analyzed by non-local density functional theory (NLDFT). The chemical composition was investigated by X-ray photoelectron spectroscopy (XPS, Thermo ESCALAB 250XI). The microstructure was characterized by transmission electron microscopy (TEM, Tecnai G2 20).

2.4. Evaluation of adsorption performance

CR solutions were prepared to investigate the adsorption performance of the synthesized MIL-101 and ZIF-8. The adsorption kinetics studies were conducted by adding an exact amount of the adsorbents (15 mg) into the CR solutions (50 mL) with the concentrations of 10, 30 and 80 mg L⁻¹ without any pH adjustment. The CR solutions containing the adsorbents were stirred using magnetic stirrers and maintained for a fixed time between 1 and 60 min at 298 K. After adsorption for a pre-determined time, the solution was separated from the adsorbents with a syringe filter (glass fiber, 0.45 μ m) and analyzed. The adsorption isotherm studies were carried out in batch mode. A series of CR solutions with concentrations varying from 10 to 1500 mg L⁻¹ were prepared and placed in an incubator shaker at 150 rpm for 12 h at 298 K. For the thermodynamics study, the adsorption isotherm studies were conducted at 308 and 318 K in addition to 298 K. After

equilibrium, the concentration of the CR solutions was determined using UV-vis spectrophotometer (DR-5000, HACH) at 497 nm.

3. Results and discussion

3.1. Characterization

The powder XRD patterns of MIL-101 and ZIF-8 are shown in Fig. 1a, which are generally in agreement with previous studies [12,15]. The sharp peaks demonstrate good crystallinity of the as-synthesized MIL-101 and ZIF-8 samples. The N_2 adsorption-desorption isotherms were used to examine the pore structure of MIL-101 and ZIF-8 (Fig. 1b) and the results are given in Table S1. As evident

in Fig. 1b, MIL-101 and ZIF-8 displayed typical type-I isotherm, suggesting intrinsic microporous characteristics. Further, MIL-101 and ZIF-8 were found to have high BET surface areas of 3549 and 1591 $m^2 g^{-1}$, respectively. According to the pore size distribution plots (Fig. S1), three windows at about 1.05, 1.19 and 1.43 nm were observed for ZIF-8; while four aperture sizes at about 0.593, 1.02, 2.27 and 3.06 nm were detected for MIL-101. The textural properties of as-synthesized MIL-101 and ZIF-8 are consistent with previous reports [12,15].

SEM, TEM and XPS analyses were conducted to determine the morphology, microstructure and the chemical composition of the MIL-101 and ZIF-8 samples. As indicated in Fig. 1c, the XPS survey spectra of the samples confirm the existence of C, O and Cr elements in MIL-101, and C, N and Zn elements in ZIF-8. As evident in Fig. 1d–g, MIL-101

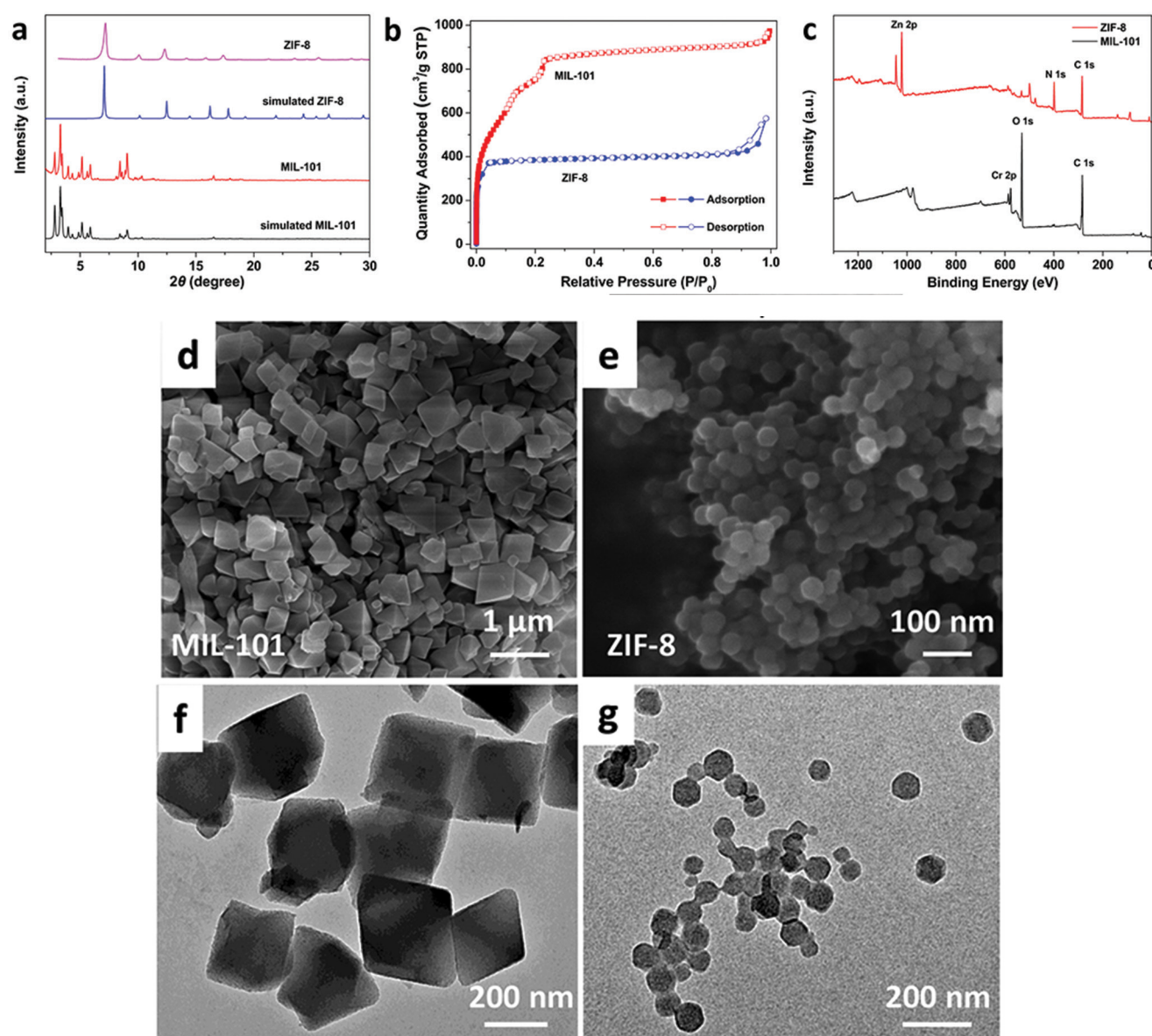


Fig. 1. (a) XRD patterns, (b) N_2 adsorption-desorption isotherms, (c) XPS spectra, (d and e) SEM images, and (f and g) TEM images of MIL-101 and ZIF-8.

shows well-defined octahedral shape with a size of 200–500 nm, whereas the ZIF-8 displays uniform morphologies of polyhedral nanocrystals with particle size of 40–50 nm, similar to previous studies [15,19].

3.2. Adsorption kinetics

To investigate the adsorption kinetics, the CR removal efficiencies of MIL-101 and ZIF-8 were measured at different concentrations. As shown in Fig. 2, at low CR concentrations (10 and 30 mg L⁻¹), the dyes were completely removed by the MIL-101 and ZIF-8 within the first 1 and 2 min, respectively. At the high CR concentration up to 80 mg L⁻¹, a complete removal was still achieved by MIL-101 within a short period of 5 min, while ZIF-8 nanocrystals reached the adsorption equilibrium after 40 min. However, Jiang et al. [11] reported that ZIF-8 nanoparticles took more than 100 min, indicating that the adsorbents synthesized in this study have faster uptake rate. These results suggest that MIL-101 and ZIF-8 are highly efficient for the CR adsorption, especially MIL-101.

For precise comparison of the adsorption kinetics, the adsorption data were analyzed using the pseudo-first-order and pseudo-second-order kinetic models expressed as follows:

$$\ln(q_e - q_t) = \ln q_e - k_1 t \quad (1)$$

$$\frac{t}{q_t} = \frac{1}{k_2 q_e^2} + \frac{1}{q_e} t \quad (2)$$

where q_e and q_t (mg g⁻¹) are the amount adsorbed at equilibrium and time t , respectively. The parameter k_1 (min⁻¹) and k_2 (g mg⁻¹ min⁻¹) are the kinetic rate constants of pseudo-first-order and pseudo-second-order models, respectively.

The $\ln(q_e - q_t)$ or t/q_t versus t kinetic plots are given in Fig. S2 in Supplementary Information, and Fig. 3, respectively, and the calculated parameters are given in Table 1. The pseudo second-order kinetic plots explained the data significantly better than the pseudo first-order kinetic model, with the correlation coefficient (R^2) above 0.999. Moreover, calculated q_e values from the pseudo second-order kinetics model are closer to the experimental values, suggesting that the pseudo-second-order kinetic model is more suitable for describing the CR adsorption process by MIL-101 and ZIF-8. Additionally, calculated rate constants (k_2) and adsorption amounts (q_e) of MIL-101 are larger than those of ZIF-8, indicating a higher CR adsorption performance of MIL-101.

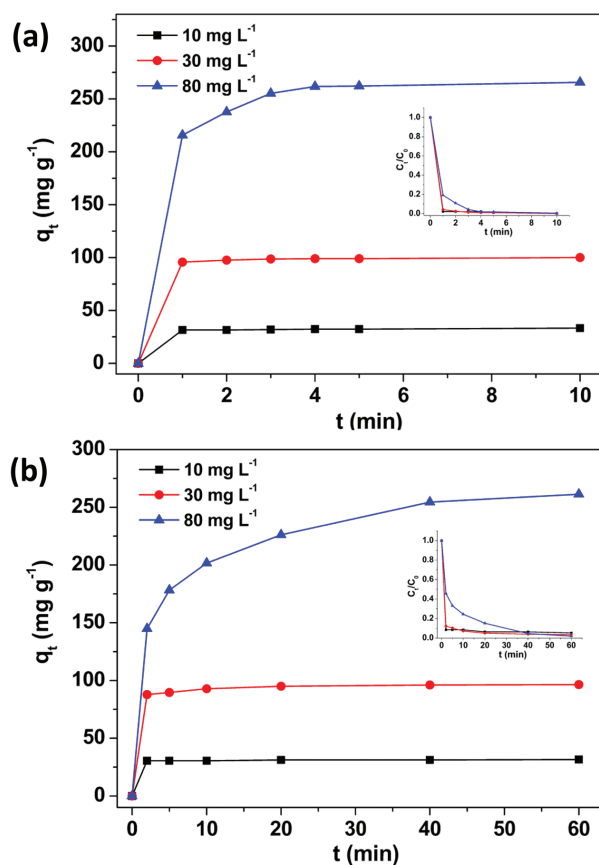


Fig. 2. Effect of contact time and initial CR concentration on adsorption of CR by (a) MIL-101 and (b) ZIF-8 adsorbents, 15 mg per 50 mL, neutral pH, 298K; the insets show the CR adsorption efficiencies of MIL-101 and ZIF-8.

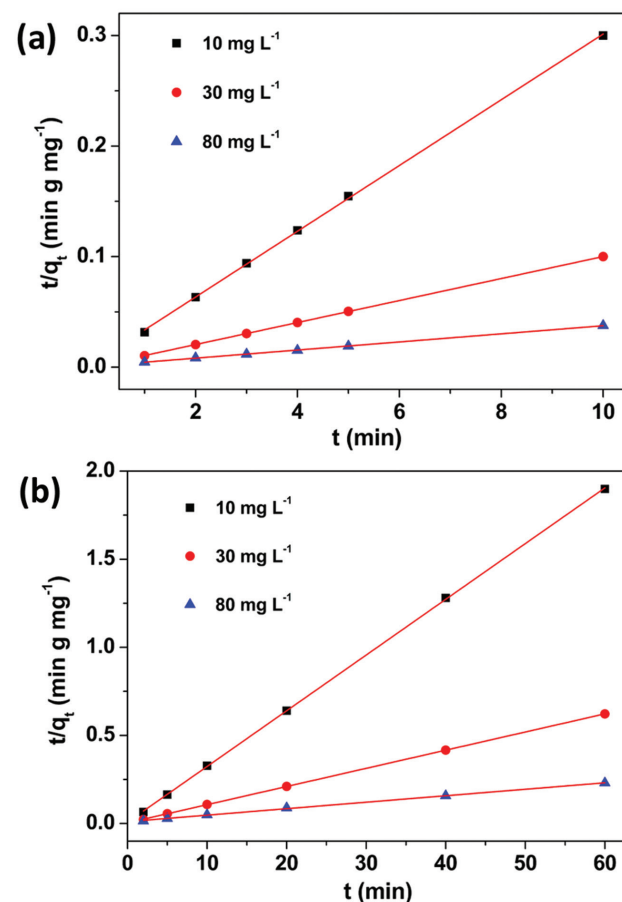


Fig. 3. Pseudo-second-order kinetics model for CR adsorption by (a) MIL-101 and (b) ZIF-8.

Table 1
Pseudo kinetic models parameters for CR adsorption by MIL-101 and ZIF-8

Sample	C_0 (mg L ⁻¹)	$q_{e,exp}$ (mg g ⁻¹)	Pseudo-first-order kinetics			Pseudo-second-order kinetics		
			$q_{e,cal}$ (mg g ⁻¹)	k_1 (min ⁻¹)	R_2	$q_{e,cal}$ (mg g ⁻¹)	k_2 (g mg ⁻¹ min ⁻¹)	R_2
MIL-101	10	33.3	2.17	0.160	0.862	33.6	0.221	0.999
	30	100	5.27	0.374	0.873	101	0.168	0.999
	80	266	101	0.722	0.942	273	0.0156	0.999
ZIF-8	10	31.6	1.17	0.0346	0.671	31.6	0.136	0.999
	30	96.5	9.33	0.0841	0.984	97.4	0.0284	0.999
	80	261	129	0.0723	0.991	272	0.00128	0.999

3.3. Adsorption isotherms

Adsorption isotherm is used to estimate the adsorption capacity of adsorbents. Thus, the equilibrium data for CR adsorption on MIL-101 and ZIF-8 were analyzed using the Langmuir and Freundlich isotherm models expressed as follows:

$$\frac{C_e}{Q_e} = \frac{C_e}{Q_m} + \frac{1}{Q_m b} \quad (3)$$

$$Q_e = K_f C_e^{1/n} \quad (4)$$

where Q_e (mg g⁻¹) is the adsorption amount at equilibrium and Q_m (mg g⁻¹) is the maximum adsorption capacity. C_e (mg L⁻¹) is the equilibrium concentration. b (L mg⁻¹) represents the Langmuir affinity constant related to the binding strength. K_f and n are constants related to the adsorption capacity and intensity, respectively.

Fig. 4 presents the isotherms for CR adsorption on MIL-101 and ZIF-8 at 298, 308 and 318 K. The Langmuir and Freundlich plots are separately displayed in Figs. 5 and S3 in Supplementary Information, and relevant parameters for both models are listed in Table 2. Accordingly, the Langmuir plots describe the isotherm data better than the Freundlich model, suggesting that the adsorption of CR by MIL-101 and ZIF-8 is monolayer adsorption. As evident in Table 2, Q_m of ZIF-8 is 1381 mg g⁻¹ at 298 K, which is higher than that of newly reported ZIF-8 (1250 mg g⁻¹) at 303 K [11]. This could be due to the particle size of the latter being 0.93 μm, which is around 19 times larger than that of the former (50 nm). A similar finding has been reported by Fan et al. [20].

In the case of MIL-101, an extraordinary adsorption capacity (Q_m) of 2248 mg g⁻¹ was achieved at 298 K, relatively superior to MIL-101 synthesized by hydrofluoric acid-free method [18]. Moreover, the maximum adsorption capacities of MIL-101 and ZIF-8 samples were compared with those of other reported adsorbents (Table 3). It is seen that the adsorption capacities of the as-prepared samples in our study are significantly higher than those of most reported adsorbents [21–27]. Especially, the Q_m of MIL-101 is closer to the largest value of 2429 mg g⁻¹ at 300 K, previously reported by Xiao et al. [27], further demonstrating the

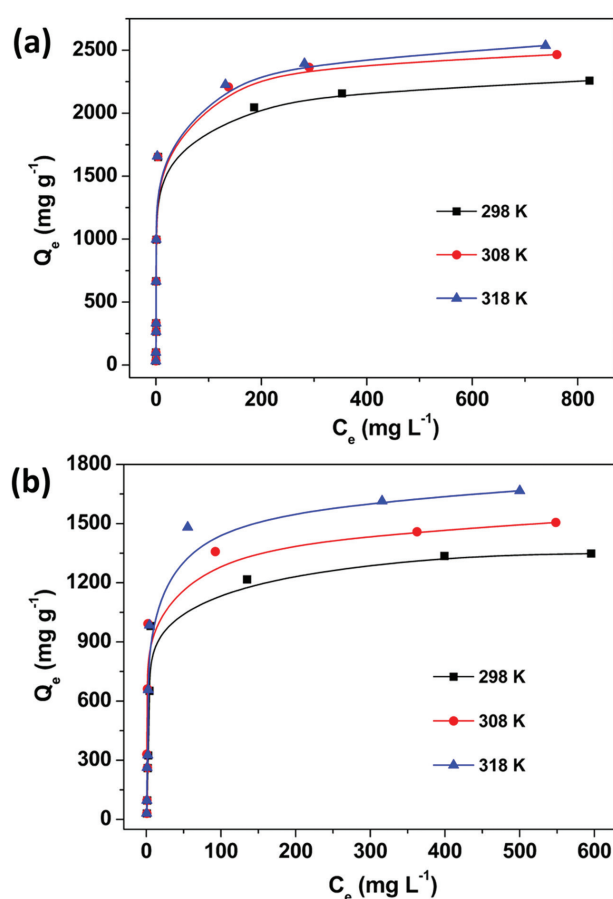


Fig. 4. Adsorption isotherms for the CR adsorption by (a) MIL-101 and (b) ZIF-8 adsorbents, 30 mg per 100 mL, neutral pH.

excellent adsorption performance of the as-prepared MIL-101 in this study.

3.4. Adsorption thermodynamics

Thermodynamic studies can provide important information about the inherent energetic changes involved in the adsorption process. Thermodynamic equilibrium

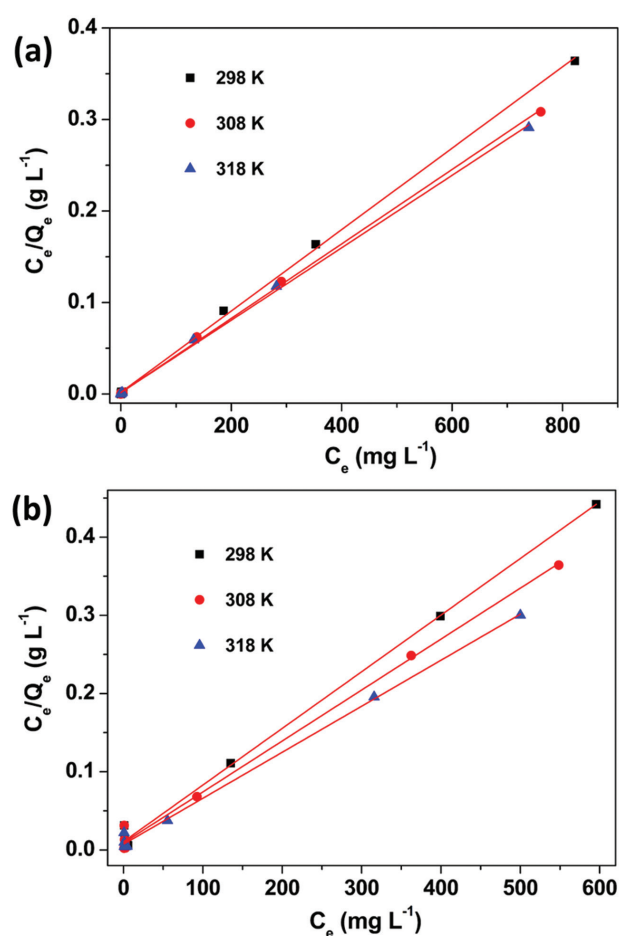


Fig. 5. Langmuir adsorption isotherms plots for (a) MIL-101 and (b) ZIF-8.

constant K_0 and Gibbs free energy change ΔG (kJ mol^{-1}) for the CR adsorption on MIL-101 and ZIF-8 can be calculated by the following equations:

$$K_0 = \frac{Q_e}{C_e} \quad (5)$$

Table 3

Comparison of the maximum CR adsorption capacities of various adsorbents

Type of adsorbent	Q_{max} (mg/g)	Reference
MIL-101	2248	This work
ZIF-8	1381	This work
CoFe_2O_4 (S5)	241.5	[21]
Mesoporous ZrO_2 fibers	103.46	[22]
Hierarchical porous ZnO microspheres	334	[23]
Ni/Mg/Al layered double hydroxides	1250	[24]
Hierarchical NiO-SiO ₂ composite hollow microspheres	204.1	[25]
Flake-like NiFe_2O_4 nanoparticles	92.5	[26]
Coordination supramolecular polymer $[\text{Cu}(\text{bipy})(\text{SO}_4)]_n$	2429	[27]

$$\Delta G = -RT \ln K_0 \quad (6)$$

where Q_e (mg g^{-1}) and C_e (mg L^{-1}) are the adsorption amount and concentration at equilibrium, respectively. R is universal gas constant and T (K) is the temperature. The values of K_0 were obtained from $\ln(Q_e/C_e)$ versus Q_e plot and by extrapolating Q_e to zero (Fig. S4) [10]. Table 4 shows negative ΔG values, indicating the spontaneous CR adsorption by MIL-101 and ZIF-8.

The enthalpy change ΔH (kJ mol^{-1}) and entropy change ΔS ($\text{J mol}^{-1} \text{K}^{-1}$) can be calculated using the following Van't Hoff equation:

$$\ln b = \frac{\Delta S}{R} - \frac{\Delta H}{RT} \quad (7)$$

The positive values of ΔH , calculated from the Van't Hoff plots (Fig. 6), suggest that the CR adsorption process

Table 2
Isotherms parameters for CR adsorption by MIL-101 and ZIF-8

Sample	T (K)	Langmuir model			Freundlich model		
		Q_m (mg g^{-1})	b (L mg^{-1})	R_2	K_F	n	R_2
MIL-101	298	2248	0.251	0.999	518	3.56	0.852
	308	2459	0.295	0.999	559	3.43	0.865
	318	2526	0.264	0.999	599	3.46	0.855
ZIF-8	298	1381	0.0687	0.997	146	2.41	0.573
	308	1535	0.0725	0.994	203	2.79	0.430
	318	1700	0.0816	0.996	176	2.27	0.603

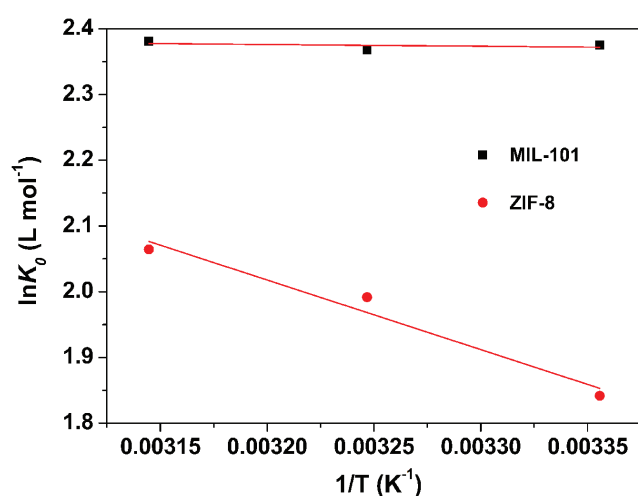


Fig. 6. Van't Hoff plots for CR adsorption over MIL-101 and ZIF-8.

Table 4

Thermodynamic parameters for CR adsorption by MIL-101 and ZIF-8

Sample	T (K)	K_0	ΔG (kJ mol ⁻¹)	ΔH (kJ mol ⁻¹)	ΔS (J mol ⁻¹ K ⁻¹)
MIL-101	298	10.75	-5.885	0.2193	20.59
	308	10.68	-6.064		
	318	10.82	-6.295		
ZIF-8	298	6.307	-4.563	8.812	44.90
	308	7.327	-5.099		
	318	7.881	-5.458		

by MIL-101 and ZIF-8 was an endothermic reaction, which is consistent with the trends observed in Fig. 4, i.e., the adsorption capacity increased with increasing temperature. ΔS represents the disorderliness of the CR molecules on MIL-101 and ZIF-8. Therefore, it can be concluded that the adsorption of CR on ZIF-8 had higher randomness (higher positive ΔS) than CR on MIL-101.

3.5. Regeneration and reuse

The reusability of the adsorbents is a critical factor for practical application. In this study, five consecutive regeneration cycles with ethanol as the regeneration agent were carried out to evaluate the reusability of MIL-101 and ZIF-8. As shown in Fig. 7, the adsorption capacity of ZIF-8 remained about the same after five cycles. However, the adsorption capacity of MIL-101 declined during the first three cycles, which may be attributed to the chemical adsorption in the process. In the case of MIL-101, numerous potentially unsaturated chromium sites exist in the framework upon the removal of coordinated water molecules [28], while the metal ions in the framework of ZIF-8 are coordinatively saturated

[29]. The Cr(III) unsaturated metal sites in MIL-101 can coordinate with the amine groups in CR to form coordination complexes. The CR molecules absorbed by coordination cannot be easily eluted, leading to the loss of adsorption capacity of MIL-101. Nevertheless, adsorption capacity of MIL-101 was still high at around 2000 mg g⁻¹ even after five cycles, suggesting good regenerability and reusability of MIL-101 and ZIF-8 and their potential in practical applications.

3.6. Adsorption mechanism

As shown in Figs. 2 and 4, MIL-101 showed faster kinetics and larger capacity for the CR adsorption in comparison to ZIF-8. This can be attributed to the high porosity of MIL-101, as the adsorption capacity generally increases with increasing porosity of the adsorbents [30,31]. Importantly, pore size and pore availability are the key factors for the efficient adsorption of CR. Since the molecular size of CR is 2.66 nm [11], which is significantly larger than the pore size of ZIF-8, CR could not enter the pores of ZIF-8 and then only surface adsorption occurred. For MIL-101, large pores of 3.06 nm are accessible for the CR adsorption, leading to its better adsorption performance. Additionally, direct coordination between MIL-101 and CR is another reason for highly efficient removal of CR by MIL-101. The nitrogen lone pair electrons on the amine group in CR can interact with the Cr(III) metal sites in the MIL-101 framework. Similar finding has been reported by Man et al. and Shu et al. [32,33]. Electrostatic interaction can be other possible adsorption mechanism since the surface of MIL-101 and ZIF-8 is positively charged at neutral pH [16,17], which is the experimental condition in this study. Therefore, MIL-101 and ZIF-8, which have positive charges, may electrostatically interact with the negatively charged sulfonic acid groups in anionic CR molecules, similar to the interaction of CR with Cu₂O [33]. In addition, it is possible that π - π interactions exist between the phenyl rings of MIL-

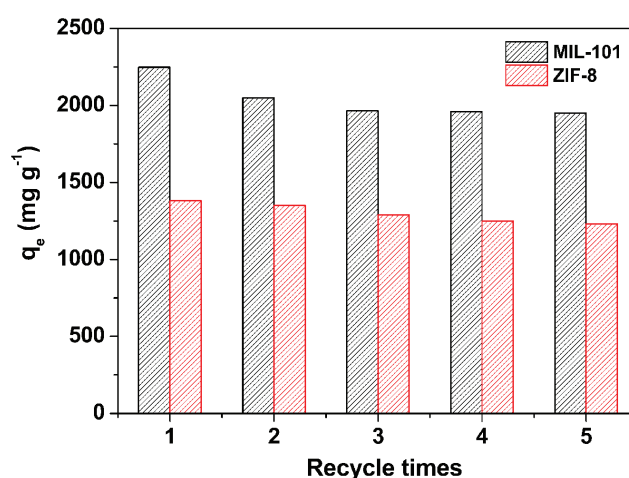


Fig. 7. Recycling of MIL-101 and ZIF-8 for the removal of CR (dosage of the adsorbents, 0.3 g L⁻¹; CR, 800 mg L⁻¹; natural pH; 298 K).

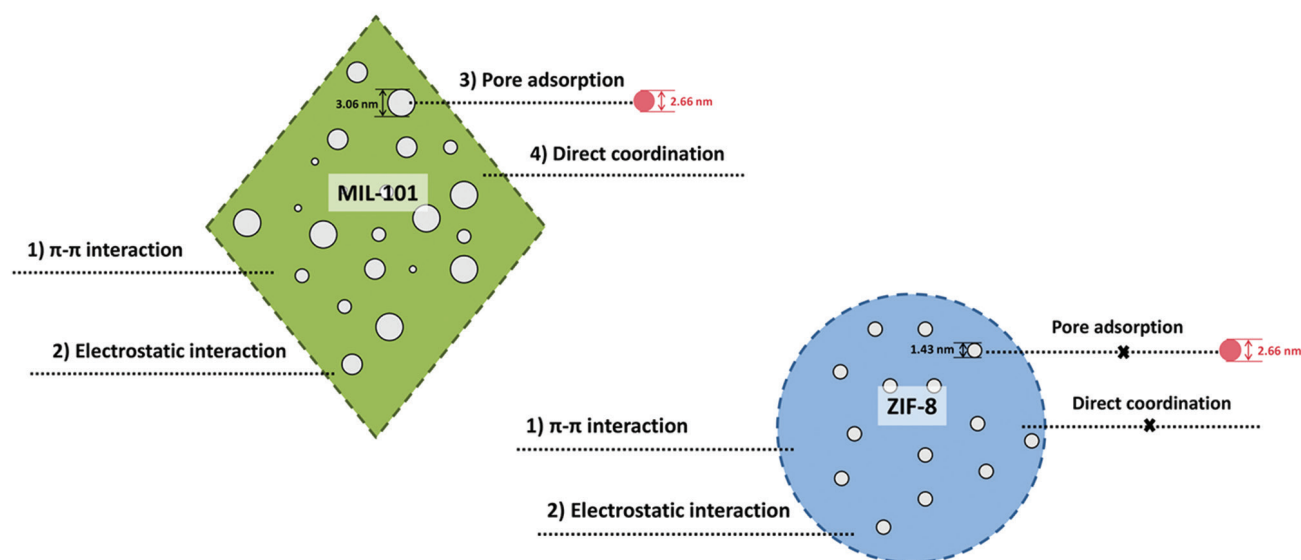


Fig. 8. Schematic diagram of the adsorption mechanisms on the MIL-101 and ZIF-8.

101 or the aromatic imidazole rings of ZIF-8 and the benzene rings of CR. Accordingly, the adsorption mechanisms of MIL-101 and ZIF-8 are given in Fig. 8.

4. Conclusions

Well-defined MIL-101 octahedrons and ZIF-8 nanocrystals were successfully synthesized through the simple one-pot routes, and were used for the CR adsorption. The study found that highly efficient removal of CR at neutral pH can be achieved with short contact time. Moreover, it was found that the adsorption performance of MIL-101 and ZIF-8 in this study was better than that of MIL-101 and ZIF-8 prepared via different methods in the previous studies. The maximum CR adsorption capacities of MIL-101 and ZIF-8 were 2248 and 1381 mg g⁻¹ at 298 K, respectively, significantly higher than most adsorbents previously studied. The CR adsorption process of the two adsorbents followed the Langmuir isotherm and pseudo-second-order kinetic models. Thermodynamic studies found that the CR adsorption onto the two adsorbents was a spontaneous and endothermic reaction. Furthermore, MIL-101 and ZIF-8 possessed good regenerability and reusability. Therefore, the study indicated that MIL-101 and ZIF-8 may be promising adsorbents for the removal of aqueous organic contaminants.

Acknowledgments

This work was supported by the Fundamental Research Funds for the Central Universities (No. 2017ZD068), the National Natural Science Fund of China (Foundation of Guangdong Province of China; No. U1401235), and the Provincial Science and Technology Planning (Guangdong Province of China; No. 2016B020240005).

References

- [1] L. Ma, W.X. Zhang, Enhanced biological treatment of industrial wastewater with bimetallic zero-valent iron, *Environ., Sci., Technol.*, 42 (2008) 5384–5389.
- [2] C.H. Huang, K.P. Chang, H.D. Ou, Y.C. Chiang, C.F. Wang, Adsorption of cationic dyes onto mesoporous silica, *Micropor., Mesopor., Mater.*, 141 (2011) 102–109.
- [3] A.A. Ahmad, B.H. Hameed, Fixed-bed adsorption of reactive azo dye onto granular activated carbon prepared from waste, *J., Hazard., Mater.*, 175 (2010) 298–303.
- [4] S. Eftekhari, A. Habibi-Yangjeh, S. Sohrabnezhad, Application of AIMCM-41 for competitive adsorption of methylene blue and rhodamine B: Thermodynamic and kinetic studies, *J., Hazard., Mater.*, 178 (2010) 349–355.
- [5] T.A. Arica, E. Ayas, M.Y. Arica, Magnetic MCM-41 silica particles grafted with poly(glycidylmethacrylate) brush: Modification and application for removal of direct dyes, *Micropor. Mesopor. Mater.*, 243 (2017) 164–175.
- [6] U. Habiba, T.A. Siddique, T.C. Joo, A. Salleh, B.C. Ang, A.M. Afifi, Synthesis of chitosan/polyvinyl alcohol/zeolite composite for removal of methyl orange, Congo red and chromium(VI) by flocculation/adsorption, *Carbohydr. Polym.*, 157 (2017) 1568–1576.
- [7] H.J. Kumari, P. Krishnamoorthy, T.K. Arumugam, S. Radhakrishnan, D. Vasudevan, An efficient removal of crystal violet dye from waste water by adsorption onto TLAC/Chitosan composite: A novel low cost adsorbent, *Int. J., Biol., Macromol.*, 96 (2017) 324–333.
- [8] S.E. Moradi, S. Dadfarnia, A.M.H. Shabani, S. Emami, Removal of congo red from aqueous solution by its sorption onto the metal organic framework MIL-100(Fe): Equilibrium, kinetic and thermodynamic studies, *Desal. Water Treat.*, 56 (2015) 709–721.
- [9] S. Lin, Z. Song, G. Che, A. Ren, P. Li, C. Liu, J. Zhang, Adsorption behavior of metal-organic frameworks for methylene blue from aqueous solution, *Micropor. Mesopor. Mater.*, 193 (2014) 27–34.
- [10] L.N. Jin, X.Y. Qian, J.G. Wang, H. Aslan, M. Dong, MIL-68 (In) nano-rods for the removal of Congo red dye from aqueous solution, *J. Colloid Interface Sci.*, 453 (2015) 270–275.
- [11] C. Jiang, B. Fu, H. Cai, T. Cai, Efficient adsorptive removal of Congo red from aqueous solution by synthesized zeolitic

- imidazolate framework-8, *Chem. Speciation Bioavailability*, 28 (2016) 199–208.
- [12] G. Ferey, C. Mellot-Draznieks, C. Serre, F. Millange, J. Dutour, S. Surble, I. Margiolaki, A chromium terephthalate-based solid with unusually large pore volumes and surface area, *Science*, 309 (2005) 2040–2042.
- [13] J. Shi, Z. Zhao, Q. Xia, Y. Li, Z. Li, Adsorption and diffusion of ethyl acetate on the chromium-based metal-organic framework MIL-101, *J. Chem., Eng., Data*, 56 (2011) 3419–3425.
- [14] K.S. Park, Z. Ni, A.P. Cote, J.Y. Choi, R. Huang, F.J. Uribe-Romo, H.K. Chae, M. O’Keeffe, O.M. Yaghi, Exceptional chemical and thermal stability of zeolitic imidazolate frameworks, *Proc., Natl., Acad., Sci., USA*, 103 (2006) 10186–10191.
- [15] L. Zhang, Z. Su, F. Jiang, L. Yang, J. Qian, Y. Zhou, W. Li, M. Hong, Highly graphitized nitrogen-doped porous carbon nanopolyhedra derived from ZIF-8 nanocrystals as efficient electrocatalysts for oxygen reduction reactions, *Nanoscale*, 6 (2014) 6590–6602.
- [16] K. Liu, S. Zhang, X. Hu, K. Zhang, A. Roy, G. Yu, Understanding the adsorption of PFOA on MIL-101(Cr)-based anionic-exchange metal-organic frameworks: Comparing DFT calculations with aqueous sorption experiments, *Environ. Sci. Technol.*, 49 (2015) 8657–8665.
- [17] N.A. Khan, B.K. Jung, Z. Hasan, S.H. Jhung, Adsorption and removal of phthalic acid and diethyl phthalate from water with zeolitic imidazolate and metal-organic frameworks, *J. Hazard., Mater.*, 282 (2015) 194–200.
- [18] Y.F. Huang, Y.Q. Wang, Q.S. Zhao, Y. Li, J.M. Zhang, Facile in situ hydrothermal synthesis of Fe_3O_4 @MIL-101 composites for removing textile dyes, *Rsc Adv.*, 4 (2014) 47921–47924.
- [19] X. Sun, Q. Xia, Z. Zhao, Y. Li, Z. Li, Synthesis and adsorption performance of MIL-101(Cr)/graphite oxide composites with high capacities of n-hexane, *Chem., Eng., J.*, 239 (2014) 226–232.
- [20] X. Fan, W. Wang, W. Li, J. Zhou, B. Wang, J. Zheng, X. Li, Highly porous ZIF-8 nanocrystals prepared by a surfactant mediated method in aqueous solution with enhanced adsorption kinetics, *ACS Appl. Mater. Interfaces*, 6 (2014) 14994–14999.
- [21] X. Wu, W. Wang, F. Li, S. Khaimanov, N. Tsidaeva, M. Lahoubi, PEG-assisted hydrothermal synthesis of CoFe_2O_4 nanoparticles with enhanced selective adsorption properties for different dyes, *Appl., Surf., Sci.*, 389 (2016) 1003–1011.
- [22] Z. Yu, B. Liu, H. Zhou, C. Feng, X. Wang, K. Yuan, X. Gan, L. Zhu, G. Zhang, D. Xu, Mesoporous ZrO_2 fibers with enhanced surface area and the application as recyclable absorbent, *Appl., Surf., Sci.*, 399 (2017) 288–297.
- [23] C. Lei, M. Pi, C. Jiang, B. Cheng, J. Yu, Synthesis of hierarchical porous zinc oxide (ZnO) microspheres with highly efficient adsorption of Congo red, *J., Colloid Interface Sci.*, 490 (2017) 242–251.
- [24] C. Lei, X. Zhu, B. Zhu, C. Jiang, Y. Le, J. Yu, Superb adsorption capacity of hierarchical calcined Ni/Mg/Al layered double hydroxides for Congo red and Cr(VI) ions, *J., Hazard., Mater.*, 321 (2017) 801–811.
- [25] C. Lei, X. Zhu, B. Zhu, J. Yu, W. Ho, Hierarchical NiO-SiO₂ composite hollow microspheres with enhanced adsorption affinity towards Congo red in water, *J., Colloid Interface Sci.*, 466 (2016) 238–246.
- [26] W. Wang, Z. Ding, S. Wu, F. Li, J.P. Liu, Ethanol-assisted synthesis and adsorption property of flake-like NiFe_2O_4 nanoparticles, *Ceram., Int.*, 41 (2015) 13624–13629.
- [27] L. Xiao, Y. Xiong, S. Tian, C. He, Q. Su, Z. Wen, One-dimensional coordination supramolecular polymer $\text{Cu}(\text{bipy})(\text{SO}_4)_{(n)}$ as an adsorbent for adsorption and kinetic separation of anionic dyes, *Chem., Eng., J.*, 265 (2015) 157–163.
- [28] Y.K. Hwang, D.Y. Hong, J.S. Chang, S.H. Jhung, Y.K. Seo, J. Kim, A. Vimont, M. Daturi, C. Serre, G. Ferey, Amine grafting on coordinatively unsaturated metal centers of MOFs: Consequences for catalysis and metal encapsulation, *Angew., Chem., Int., Ed.*, 47 (2008) 4144–4148.
- [29] H. Liu, Y. Li, H. Jiang, C. Vargas, R. Luque, Significant promoting effects of Lewis acidity on Au-Pd systems in the selective oxidation of aromatic hydrocarbons, *Chem., Commun., (Camb)*, 48 (2012) 8431–8433.
- [30] V. Fierro, V. Torne-Fernandez, D. Montane, A. Celzard, Adsorption of phenol onto activated carbons having different textural and surface properties, *Micropor., Mesopor., Mater.*, 111 (2008) 276–284.
- [31] E. Haque, N.A. Khan, S.N. Talapaneni, A. Vinu, J. Jegal, S.H. Jhung, Adsorption of phenol on mesoporous carbon CMK-3: Effect of textural properties, *Bull., Korean Chem., Soc.*, 31 (2010) 1638–1642.
- [32] I.C. Man, G. origa, V. Pârvulescu, Theoretical study of the adsorption of bromobenzene and aniline on $\text{Cu}_2\text{O}(110)$: CuO and $\text{Cu}_2\text{O}(111)$: CuO surfaces, *Chem., Phys., Lett.*, 604 (2014) 38–45.
- [33] J. Shu, Z. Wang, Y. Huang, N. Huang, C. Ren, W. Zhang, Adsorption removal of Congo red from aqueous solution by polyhedral Cu_2O nanoparticles: Kinetics, isotherms, thermodynamics and mechanism analysis, *J., Alloys Compd.*, 633 (2015) 338–346.

Supplementary Information

Table S1

Pore structure parameters of MIL-101 and ZIF-8

Sample	SBET ($\text{m}^2 \text{g}^{-1}$)	S_{Langmuir} ($\text{m}^2 \text{g}^{-1}$)	V_{pore} ($\text{cm}^3 \text{g}^{-1}$)
MIL-101	3549	4937	1.483
ZIF-8	1591	2084	0.3572

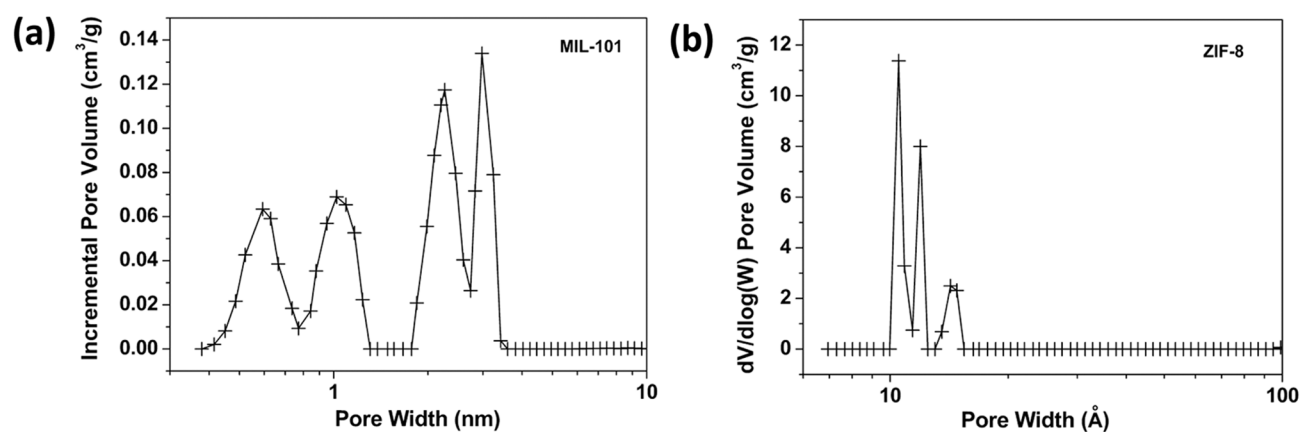


Fig. S1. Pore size distribution plots of (a) MIL-101 and (b) ZIF-8.

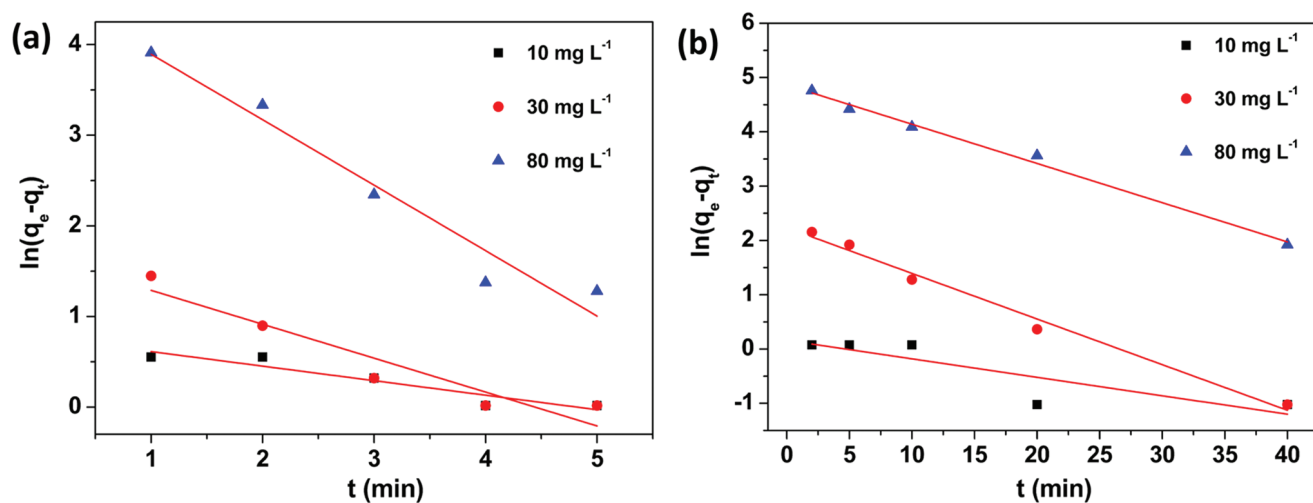


Fig. S2. Plots of pseudo-first-order kinetics of CR adsorption over (a) MIL-101 and (b) ZIF-8.

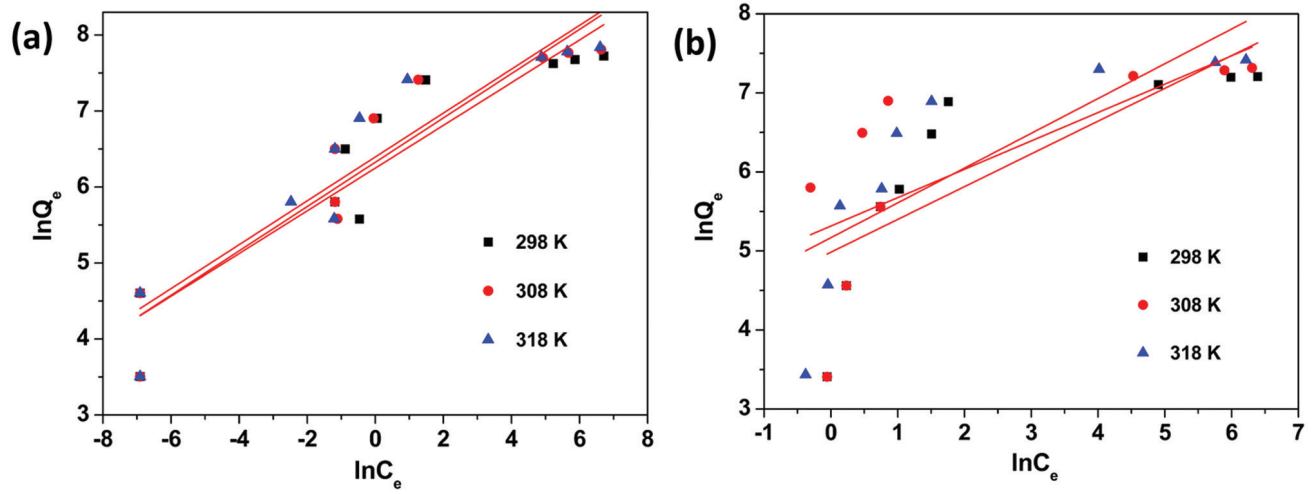


Fig. S3. Freundlich plots of the adsorption isotherms for (a) MIL-101 and (b) ZIF-8.

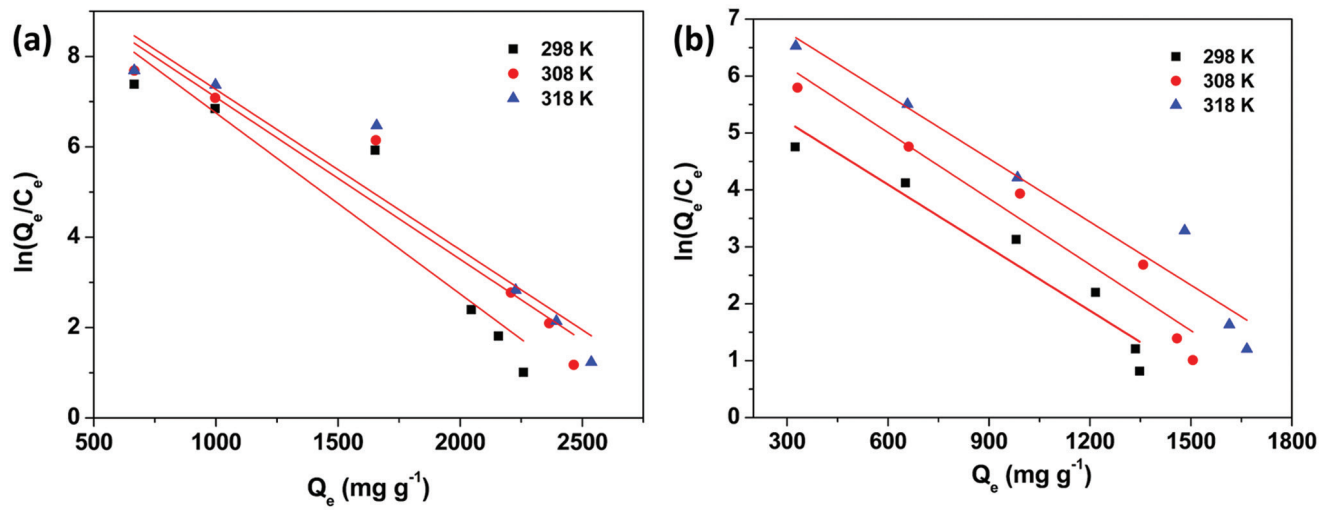


Fig. S4. Plots of $\ln(Q_e/C_e)$ vs. Q_e for CR adsorption by (a) MIL-101 and (b) ZIF-8.